

Instrument Science Report WFC3 2009-05

# The Photometric Calibration of WFC3: SMOV and Cycle 17 Observing Plan

---

J. S. Kalirai, S. Deustua, S. Baggett, R. Bohlin, T. Brown, J. MacKenty, P. McCullough,  
A. Rajan, A. Riess, E. Sabbi (STScI), & M. Sirianni (ESA)

June 11, 2009

---

## ABSTRACT

*The newly installed Wide Field Camera 3 on the Hubble Space Telescope will be extensively used by GOs during Cycle 17 for imaging astrophysical phenomena in the UV, optical, and IR. During SMOV4 and Cycle 17, the WFC3 Instrument Team will measure the photometric performance of both the UVIS and IR cameras. These observations will target a set of bright spectrophotometric standard stars and two nearby star clusters. We describe the observational strategy to measure the photometric zeropoints of all filters and the transformation equations to relate the fluxes of objects measured in these filters to other popular ground and space based systems. A detailed discussion of the rationale for the choice of targets, and the analysis plan, are also presented.*

---

## Introduction – The Hubble Space Telescope and Servicing Mission 4

The Hubble Space Telescope (HST) has served as the world's benchmark for astronomical research for almost two decades. The first of its kind, the UV/optical/NIR telescope has successfully been serviced through four manned missions in December 1993, February 1997, December 1999, and March 2002, which continuously provided it with cutting edge new technology to meet the rapidly changing needs of professional astronomy. As a direct result of these servicing missions, Hubble's ability to answer the most fundamental questions of the Universe, from our understanding of planetary science to cosmology, has always been at the competitive forefront of astronomical missions.

WFC3 was installed during the May 2009 servicing mission, replacing the extraordinarily successful WFPC2. The new WFC3 instrument will improve HST's sensitivity by over an order of magnitude, enabling the undertaking of exciting new scientific research projects. The versatility of the WFC3 instrument is particularly exciting as it provides sensitive, wide-field imaging in the UV, optical, and NIR within a single orbit. The instrument will immediately become the workhorse of the HST, carrying half of the total Cycle 17 approved orbit allocation, more than a factor of two higher than the next busiest instrument (ACS). WFC3 will be used as the primary instrument in a diverse range of studies from the characterization of low mass brown dwarfs and planets, to understanding the formation of stars and galaxies, to measuring the expansion rate of the Universe. In this document, we describe the procedures that will be undertaken to understand the photometric performance of WFC3.

### The Wide Field Camera 3

WFC3 is a new instrument containing both optical/UV CCDs and a near-infrared HgCdTe detector array, providing high-resolution imaging over the wavelength range extending from 200 nm to 1700 nm. The UVIS channel contains two CCDs that subtend an angular field of view of  $162 \times 162$  arcseconds and pixels that are 0.04 arcseconds. The IR channel contains a single detector with a field of view of  $123 \times 136$  arcseconds and pixels that subtend 0.13 arcseconds.

The complement of filters on WFC3 is substantial. There are 48 filter slots on the UVIS side that include 6 long pass and very wide filters, 12 broadband filters, 8 medium-band filters, and 36 narrow-band filters (20 of which are arranged on five quad slots). In addition to these 62 imaging filters, a UV grism is also included. On the IR side, there are 5 broadband filters, 4 medium-band filters, 6 narrow-band filters and two grisms.

The primary use of WFC3 as an HST instrument will involve imaging observations of astrophysical phenomena in these filters. Linking these observations to scientific results requires an understanding of the photometric performance of the instrument. To accomplish this global task the specific goals for the SMOV4 and Cycle 17 observing program are:

- To measure the photometric zeropoints<sup>1</sup> for the 53 WFC3/UVIS filters requested by observers in Cycle 17, and for all 15 of the WFC3/IR filters. The zeropoints will be measured on both CCDs of the UVIS camera. We aim to achieve 1% precision in the 18 broadband filters, and 2-3% accuracy in the medium and narrow-band filters on the UVIS channel. Our goal is also to reach the same level of accuracy in the IR filters, although, it remains to be seen if this can be achieved within the limits of the count and count-rate linearity corrections.

<sup>1</sup>The photometric zeropoint of a filter is defined to be the magnitude of a star-like object that produces one count per second within the photometric aperture.

- To characterize the photometric stability of the instrument, as functions of both position and time.
- To test the filter bandpasses and the quantum efficiency of the CCD detectors by repeating the zeropoint measurements on cooler stars with a different spectral energy distribution (see Bohlin 2007).
- To compute transformation equations between WFC3 broadband filters and other popular photometric systems (e.g., Johnson-Cousins, SDSS, ACS).
- To obtain  $<1\%$  relative photometric precision with respect to other HST instruments in the most requested broadband filters.

In the following sections we outline an observational plan that will be executed with the newly installed WFC3 instrument to accomplish these goals. First, we present some background and justification for the target selection process. The general observations described below fall into two broad categories. The instrument will be first commissioned during the Servicing Mission Orbital Verification (SMOV) phase, which lasts approximately 10 – 12 weeks. These data represent the first set of (in-orbit) observations to measure the performance of WFC3. Following this, a more detailed program will be executed during Cycle 17 to fully characterize the instrument. We end with a brief discussion of the analysis of these data to accomplish our goals. The presentation here reflects our overall strategy and prioritization, and does not distinguish between actual observations that will be executed in Cycle 17. The specifics of that depend on several factors, such as the length of SMOV, target visibility, schedulability with other programs, etc. Readers interested in a specific task (e.g., the target selection or the Cycle 17 observational plan) can easily skip to the relevant section. A summary of all observations is also presented at the end of the paper in Tables 3 (UVIS) and 4 (IR).

## Targets

### Zeropoints and Stability

The requirements outlined above impose strict criteria on the targets for this investigation. As we discuss later, our analysis plan requires measuring the total flux of a well-understood standard star and comparing that measurement to the expected count-rate from a calibration spectrum of the source. In order to measure the photometric zeropoints to a precision of less than a few percent, we require, 1.) a  $S/N > 100$  in counting statistics in each exposure, 2.) an isolated target to prevent flux contamination from a neighboring star, 3.) a target with a well calibrated spectral energy distribution, 4.) simple (black-body like) spectrum with minimal spectral features, 5.) a high visibility target. The last requirement is needed to test the zeropoints for variation over time. In addition to these, our requirement to provide a relative photometric precision of  $<1\%$  in broadband

filters that are common between WFC3 and other HST instruments suggests a preference for those targets that were used to calibrate previous generation instruments, including ACS, WFPC2, and NICMOS.

The criteria above are satisfied by hot white dwarfs. These are degenerate stars with (mostly) either shallow, well characterized hydrogen Balmer absorption lines or a featureless spectrum (depending on the temperature of the star). A summary of several spectrophotometric standards, including white dwarfs, that have been observed with HST are listed on the STScI CALSPEC webpage,<sup>2</sup> see Bohlin, Dickinson, & Calzetti (2001) and references therein for more information. Although some of the hotter FEIGE stars in this list exhibit a nice featureless spectrum, they have not been extensively studied by HST and modeled to the precision that we require (<1% accuracy in the flux calibration). The combined requirements listed above uniquely point to the white dwarfs G191-B2B, GD 153, and GD 71, which have been well studied by STIS, WFPC2, ACS, and NICMOS (Bohlin, Colina, & Finley 1995; Bohlin 1996; Bohlin 2000; Bohlin, Dickinson, & Calzetti 2001).

Given WFC3's broad spectral coverage in the UV and IR, our spectrophotometric standards must have a well understood absolute spectral energy calibration over a wavelength range extending from 200 nm to 1700 nm. In Figure 1, we illustrate the observed STIS spectra of G191-B2B, GD 153, and GD 71, taken from the CALSPEC database (see R. Bohlin references earlier). (The spectrum of a solar analog, P330E, is also shown and discussed later). The white dwarf spectra are plotted from 200 nm to 1000 nm, and all show the hydrogen Balmer absorption lines. The flux longward of 1000 nm falls off like a simple blackbody and is not shown for clarity. Most white dwarfs have a very simple structure, with a carbon-oxygen degenerate core and a thin hydrogen layer on the surface. Bergeron, Saffer, & Liebert (1992) have developed a widely adopted technique for measuring the parameters of a white dwarf (e.g., temperature –  $T_{\text{eff}}$  and surface gravity –  $\log g$ ) through the modeling of the observed Balmer lines in the stellar spectra. Excellent model atmosphere fits can be achieved if the Balmer lines from  $H\beta$  to the higher order transitions (e.g., H8 and H9) are well characterized ( $S/N > 50$  per resolution element), as is certainly the case for the spectra of these bright stars. Both LTE and NLTE models have been fit to these absorption lines to yield the individual parameters of each star, and the resulting model fit can be extrapolated to any wavelength to yield the spectral energy distribution of the star.<sup>3</sup> We note that the method of measuring the parameters of white dwarfs from spectroscopic model atmosphere fits has been cross-checked with independent techniques (e.g, gravitational redshifts and astrometric data) and shown to be in good agreement (Bergeron, Liebert, & Fulbright 1995; Reid 1996). Further details on the specific fits to the Balmer lines of these stars, and a comparison to broadband photometry, are provided in Bohlin (2000) and Bohlin, Dickinson, & Calzetti (2001).

<sup>2</sup><http://www.stsci.edu/hst/observatory/cdbs/calspec.html>

<sup>3</sup>The spectra and the model fits are both available at [ftp://ftp.stsci.edu/cdbs/current\\_calspec](ftp://ftp.stsci.edu/cdbs/current_calspec)

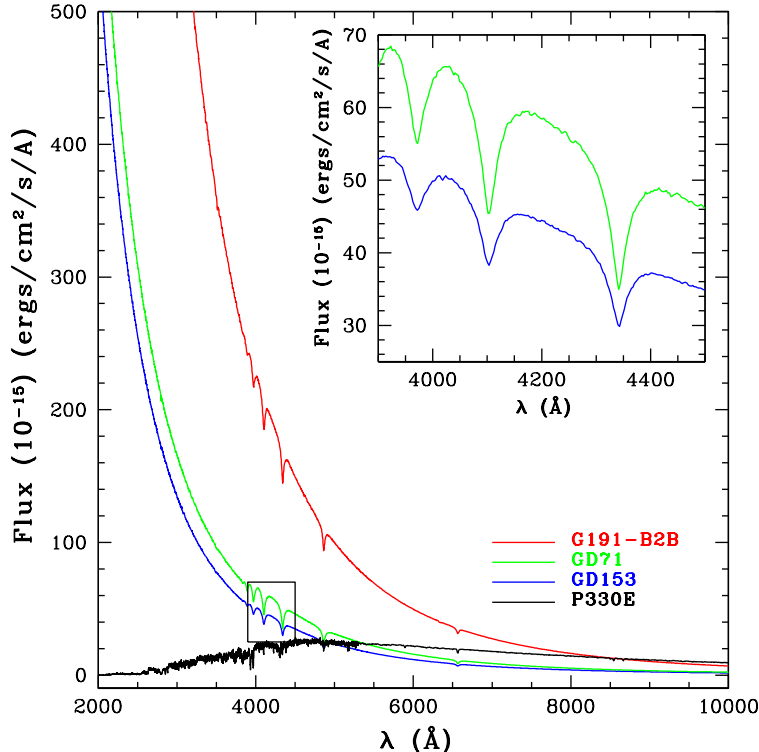


Fig. 1.— The spectra of G191-B2B (red), GD 153 (blue), GD 71 (green), and P330E (black) are shown relative to one another. The white dwarfs show a very smooth continuum with hydrogen Balmer lines. We zoom into these lines in the inset panels.

We summarize the properties of these three white dwarfs, and the solar analog P330E, in Table 1. All three of these white dwarfs are bright and hot. Although any of these stars are sufficient for our purposes and have a well constrained absolute flux calibration to an accuracy of  $<1\%$  (i.e., relative to atmosphere models), we have a slight preference for GD 153. G191-B2B, which has served as the most popular HST standard of the three, however, is a rare white dwarf whose atmosphere is significantly contaminated with heavy elements, including C, N, O, Si, Fe, and Ni (see Lanz et al. 1996). Although most of the transitions of these atomic species peak in the far-UV, there are also some lines at 200 – 300 nm, within the range of our spectral coverage. Additionally, the star is bright enough at  $V = 11.8$  that it will saturate in  $<0.5$  seconds in the WFC3 long pass filters F200LP and F350LP (the minimum exposure time due to the shutter is 0.5 seconds), and in  $<1.0$  seconds in F300X, F390W, F475W, F475X, F555W, and F606W. Although this can be mitigated by ensuring the star is not well centered on a given pixel (e.g., through a sub-pixel dither), the CCDs may perform more efficiently than the ETC currently predicts. We prefer GD 153 as it is hotter and contains shallower absorption lines than GD 71, and has a slightly better absolute flux calibration. In practice, more than one of these standards may need to be observed in Cycle 17 given their visibilities and the cadence of our observations.

We also include a redder spectrophotometric standard star, P330E, which has been observed with both ACS and NICMOS. The spectrum of this 13th magnitude star is shown in Figure 1 as a black curve. The combination of the hot white dwarf standard and this cool G dwarf will provide us with tests of the filter bandpasses and quantum efficiency of the CCDs (see Bohlin 2007). We note that GD 153, G191-B2B, and P330E will be observed by ACS in Cycle 17 for calibration purposes.<sup>4</sup>

## Photometric Transformations

The WFC3 filter set contains many analogs to popular ground and space based photometric systems, including the Johnson-Cousins, SDSS, WFPC2, Stromgren, and Washington systems. Although most observers will translate physical quantities from stellar models into the WFC3 filter system (e.g., luminosity and temperature from stellar isochrones), we nevertheless provide a limited set of transformations from WFC3 to the most popular broadband filters in these other systems. Such conversions typically involve defining a transformation equation that compares the flux in the target (other) band to the source (WFC3) band through an offset and color term (possibly second order). The coefficients of the transformation equations can be determined from a least squares fit.

Sirianni et al. (2005) summarize some of the pitfalls associated with such photometric transformations for the specific case of the ACS filters. The transformations depend on several factors including metallicity and age, and, possibly second order effects due to rotation and magnetic fields. The accuracy of the transformation is limited by differences in bandpass shape and width (e.g., a spectral feature can appear in one band but not the other) and by the number of comparison stars that are well detected in both systems. It is important to not only measure the transformation equations but also to characterize the ranges over which they are valid and the respective uncertainties (and therefore the practicality for various scientific purposes).

The need for a large set of stars to define the transformation equations naturally suggests imaging observations of well studied globular clusters. Both 47 Tuc and NGC 2419 were used by

<sup>4</sup>Cycle 17 Proposal 11889, Bohlin et al.

Table 1: Properties of Spectrophotometric Standards

Target	$B$	$V$	$J$	$H$	$T_{\text{eff}}$ (K)	$\log g$
G191-B2B	11.45	11.77	12.55	12.66	61,200	7.49
GD153	13.06	13.35	14.07	14.19	38,700	7.66
GD71	12.78	13.03	13.74	13.86	32,700	7.68
P330E	13.65	13.00	11.82	11.48	G0V	—

Sirianni et al. (2005) to determine the ACS optical transformations, because they have been well studied by WFPC2 and ACS programs, as well as ground-based *UBVRI* (Peter Stetson<sup>5</sup>) and *JHK* (for 47 Tuc) photometry. Because the clusters span a range of metallicity and distance: 47 Tuc ( $[\text{Fe}/\text{H}] = -0.70$ ,  $d = 5$  kpc) and NGC 2419 ( $[\text{Fe}/\text{H}] = -2.2$ ,  $d = 90$  kpc) together enable a sampling of the entire WFC3 wavelength range. Observations of 47 Tuc cover the color range provided by a rich main-sequence extending from the blue turnoff to faint red stars, while NGC 2419 samples both ultraviolet and blue wavelengths through the population of horizontal branch stars, and the redder part of the CMD through the rich red giant branch of the cluster (see Figure 2). We will repeat the observations of these two clusters in a subset of the primary UVIS broadband filters (described later). In the infrared, 47 Tuc will be observed through the five broadband IR filters. Additional observations of the young cluster NGC 1850, which NICMOS observed with its F110W and F160W filters, will be obtained in the WFC3 F110W and F160W filters in the WFC3 Calibration Program 11933 on the IR Rate Dependent Non-Linearity (Riess et al.). This cluster provides a calibration source to compute photometric transformations between the WFC3 IR and NICMOS filters.

## Servicing Mission Orbital Verification (SMOV) Calibration Plan

SMOV extends for roughly two months, beginning a few weeks after SM4 is completed, from June 11th to August 14th 2009. During SMOV, we will obtain preliminary observations to define the photometric zeropoints of WFC3 in 37 essential UVIS filters (16 highest priority, 20 lower priority, and 1 ERO filter).<sup>6</sup> These filters have been chosen based on usage statistics for Cycle 17. On the IR side, we will define the photometric zeropoints in all 15 filters.<sup>7</sup> An additional goal is to test for photometric stability of the instrument over a one month period.

UVIS observations consist of a series of very short exposures of GD 153 in each filter using the  $512\text{k} \times 512\text{k}$  subarray on UVIS1 (the chip with the least number of “droplet” features, see Brown,

<sup>5</sup><http://cadwww.hia.nrc.ca/cadcbn/wdb/astrocat/stetson/query>

<sup>6</sup>SMOV proposal 11450, J. Kalirai & T. Brown.

<sup>7</sup>SMOV proposal 11451, J. Kalirai & T. Brown.

Table 2: Properties of Globular Clusters for Photometric Transformations

Target	$d$ (kpc)	$[\text{Fe}/\text{H}]$	Calibration
47 Tuc	5	-0.7	ACS/WFPC2
NGC 2419	90	-2.2	ACS/WFPC2
NGC 1850	50	$\lesssim 0$	NICMOS

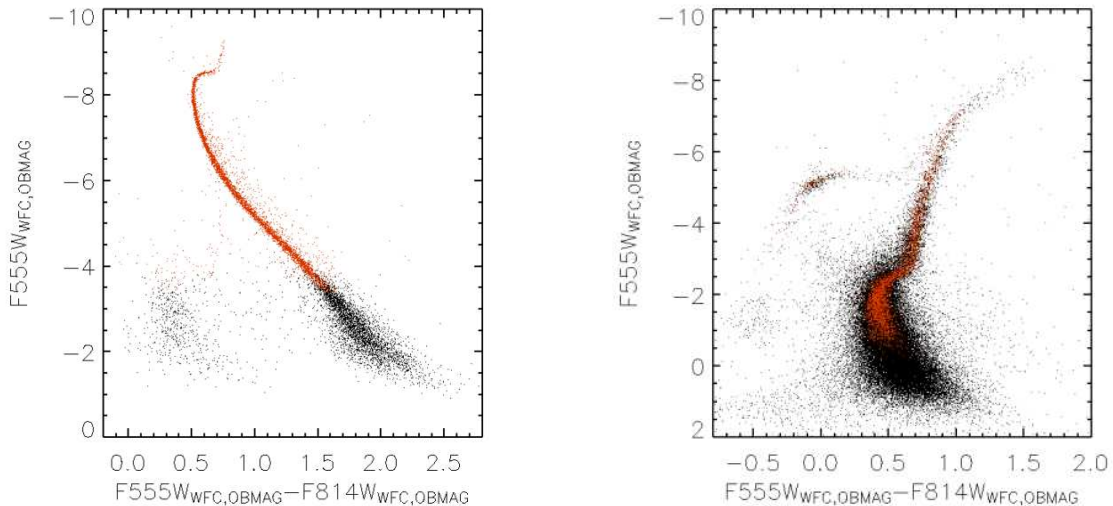


Fig. 2.— *The ACS color-magnitude diagrams of 47 Tuc (left) and NGC 2419 (right) nicely sample both bright blue and red stars over the optical colors (Note: 47 Tuc has a red clump horizontal branch and no hot horizontal branch stars). We will observe both of these clusters in a set of broadband WFC3 filters for use in defining photometric transformations between our filters and the ACS (and other space and ground based) systems.*

Hartig, & Baggett 2008). The subarray is used to reduce overhead in the readouts given the large number of exposures per orbit. A possible drawback to using the subarray is that the enclosed flux of the standard star may extend beyond the region being read out, a possibility that we address later when we discuss the analysis steps. We also adopt a four point, non-integer pixel dither pattern ( $\sim 40$  pixels) on most observations that allows us to a.) reject cosmic rays and ensure that the target does not land on the same hot pixel, b.) alleviate any saturation concerns by ensuring that the bright standard star is not centered on the pixel in at least one exposure, and c.) monitor detector variations over a small area through relative photometric comparisons.

All exposure times are selected to ensure a  $S/N > 100$  in counting statistics at each dither position for each filter in most exposures, and a  $S/N > 100$  with a coadded data set in a few narrowband and quad filters. For most filters, this  $S/N$  requires an observation of just a few seconds or shorter. The first visit will consist of five orbits to be executed early in SMOV. In order to measure the photometric stability, the observations will be repeated in a set of eight key broadband filters (F225W, F275W, F336W, F390W, F438W, F555W, F606W, F814W) at time intervals of 1 day, 1 week, and 1 month. Each of these repeat visits requires a single orbit for a total of 8 orbits to accomplish the SMOV goals.

The photometric zeropoints of the IR channel during SMOV will be defined by observing two stars with distinct temperatures, GD 153 and the solar analog P330E. We will expose all filters



initially with a RAPID sequence and then a subset of narrower filters in the SPARS10 sequence (to increase S/N). The  $128k \times 128k$  subarray will be used to reduce overheads and to scale exposure times to levels that will provide multiple samples before saturation. Two dither positions (separated by  $\sim 5$  pixels) will be used to test for detector variations and to remove cosmic rays and hot pixels. Again, the dither will be non-integer to mitigate saturation in the later reads of the sample sequence. The observations of 15 filters requires a single orbit per star, and will be repeated after 1 day, 1 week, and 1 month, for a total of 8 orbits to accomplish the SMOV goals.

We note that all three of the photometric white dwarf standards are not available all year. For example, the secondary white dwarf targets G191-B2B and GD 71 are unavailable from March 30th – July 25th 2009 and March 30th – August 10th 2009, respectively, and therefore do not fulfill the required cadence of our observations (1 month visibility during SMOV). Therefore, the primary target GD 153, must be observed. However, this star is unavailable from July 13th – November 10th 2009 and hence must be initially observed very early in SMOV to satisfy the one month repeat observations. The solar analog P330E is available all year round.

## Cycle 17 Calibration Plan

Following the initial SMOV calibration of a subset of high priority filters, we will execute a more rigorous test of the photometric performance of the WFC3 UVIS and IR channels. During these Cycle 17 observations, every filter that is being used by a GO will be calibrated.

## UVIS – Spectrophotometric Standards

Cycle 17 UVIS observations initially consist of a set of exposures of our bright white dwarf standard in 53 of the 62 UVIS filters. We will use a (subpixel) two-point dither pattern, the  $512k \times 512k$  subarray, and observe the standard star both on amp A of UVIS1 and amp C of UVIS2. The initial five orbit visit (01) will expose the standard star in all 42 of the regular broadband, medium-band, and narrow-band filters. A second visit (02) consists of a single orbit observation of the standard star in the 11 narrow-band quad filters requested in Cycle 17, using a custom defined subarray of  $1280 \times 512$  pixels with the star centered on the CCD amp where the quad filter falls. This subarray ensures that the overscan regions are included in the readout. For almost all observations, we will obtain a  $S/N > 100$  detection of the standard, the exception being a few quad filters where we will reach  $S/N \sim 100$  (adequate to measure the zeropoint to a few percent in these filters). An example of a typical orbit in this visit is given in Figure 3.

To monitor the photometric stability of WFC3 over time and position, we will repeat the standard star observations in the 15 most used Cycle 17 filters (11 broadband, 2 medium-band, 2 narrow-band, and 1 quad filter) and F850LP. A four point dither pattern, with large non-integer shifts will be adopted to move the star to different detector positions. Except for the quad filter,

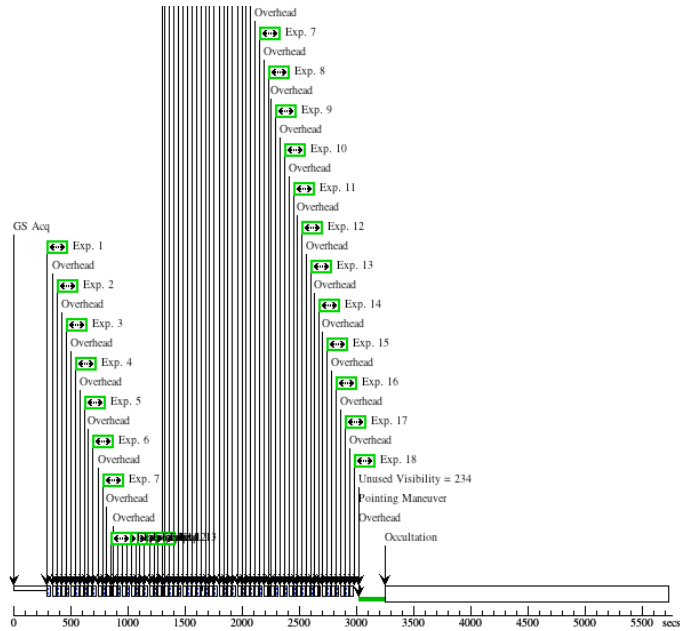


Fig. 3.— *The first orbit of the first visit in our Cycle 17 calibration plan, exposing a set of 18 filters in a two point dither pattern on the UVIS channel. Each observation spans less than a few seconds and will achieve a  $S/N > 100$  detection for GD153 in all filters.*

where we use the custom subarray developed earlier, the observations will be split between amp A on UVIS1 and amp C on UVIS2. Each of these repeat checks requires two orbits, the last exposure on each being a full chip readout. These observations will be obtained approximately 1, 2, 3, 5, 7, 9, 11, and 13 months after the start of the Cycle and are assigned visits 03 – 10 (note, the filter exposed in the full chip readout is varied at each visit, and we alternate between UVIS1 and UVIS2). These repeat observations therefore comprise 16 orbits of our program.

Observations identical to the above, for our secondary and tertiary standards G191-B2B and GD 71 are built into our proposal in case the primary target GD 153 is not available (e.g, at the beginning of the currently planned Cycle 17).

As mentioned above, G191-B2B has served as the most popular HST standard star and was used by ACS and NICMOS for photometric calibration. Although our primary purpose is to achieve a photometric calibration of 1% in the WFC3 broadband filters, an even better HST “relative” calibration may be possible by directly comparing the flux of a given star that WFC3/UVIS measures in a particular filter to what previous instruments measured. Additionally, we note that it is always safer to observe a second standard star rather than rely the entire calibration program on a single primary object. We have therefore supplemented the primary observations discussed above with a small set of G191-B2B observations, even though the star will come dangerously close to satu-

ration in some of our filters. We have selected ten of the most important broadband filters based on WFC3 and ACS usage (F336W, F350LP, F390W, F438W, F475W, F555W, F606W, F775W, F814W, F850LP), and will observe G191-B2B with very short (i.e.,  $<1$  second) exposure times using a four-point sub-pixel dither box and the  $512k \times 512k$  subarray (UVIS1-C512A-SUB). The observations will easily achieve  $S/N > 100$  at each dither position and will be initially executed at the start of the Cycle 17 calibration period (Visit 20) and then repeated four times (Visits 21 – 24), at intervals of approximately three months to monitor stability. Each visit requires one orbit for a total of four orbits. Depending on the timing of Cycle 17, the first sets of observations in this sequence can be ignored if G191-B2B becomes the primary standard.

In order to establish a color correction for the broadband filters, we also include observations of the redder spectrophotometric standard P330E, a bright well studied solar analog, in all 18 of the UVIS broadband filters and 6 of the 8 medium-band filters. Exposure times for this star vary from 0.5 to 300 seconds to reach a  $S/N > 100$ , and are executed with the  $512k \times 512k$  subarray on UVIS1 using a four point (non-integer) dither pattern. These observations require three orbits to complete and will be executed once at the start of Cycle 17 (Visit 30) and once in the middle of the Cycle (Visit 31), for a total of six orbits.

Altogether, the UVIS observations of photometric standards require an allocation of 33 orbits. In addition to this, we note that we can also leverage the observations of the white dwarf standard GRW+70D5824, which is being observed in Cycle 17 Proposal 11907 by Baggett & Borders. These observations are scheduled once per week for the first 14 weeks, and then twice per month afterwards. The bright star will be observed in 11 WFC3 filters, at two locations on the detector during each visit (see Proposal 11907 and SMOV proposal 11426).

## UVIS – Star Clusters

As discussed earlier, we will observe the two globular clusters 47 Tuc and NGC 2419 to establish photometric transformations with other photometric systems. For the UVIS channel, we will image the same field as ACS with 17 (11) of our 18 broadband and wide filters in NGC 2419 (47 Tuc). The one filter not being observed is F218W, which is too blue to detect an appreciable number of stars in a reasonable exposure time. All exposures are obtained using the full frame UVIS readout and without any dithers.

The star cluster observations are divided into three sets. The primary calibration for the bluer filters on UVIS will come from the hot horizontal branch stars of NGC 2419 ( $V_{HB} = 21$ ). We have therefore set exposure times to measure 1 magnitude below the horizontal branch with  $S/N = 10$  for F225W, F275W, F336W, F390W. The exposure times range from 5 – 15 minutes for these filters. The data for the very wide and long pass filters such as F200LP, F300X, and F350LP, with less exposure time, will reach deeper than this limit and therefore also probe the cooler part of the branch (see Figure 3). We note that the limiting number of stars along the horizontal branch of

this (or any) cluster, and the generally larger uncertainties in ground based  $U$ -band data will limit the accuracy of photometric transformations for these bands.

Next, for the set of filters that are at the wavelength, or redder, than the  $U$ -band we will also heavily rely on the horizontal branch stars of NGC 2419, however, we can also sample the luminosity function of the bluest main-sequence stars in the cluster. Therefore, we set exposures to sample the jump in the luminosity function at the turnoff ( $V = 24$ ), by ensuring a  $S/N = 10$  detection for stars that are 1 magnitude below the turnoff. These data will include observations in F438W, F475W, and F475X.

For the most popular broadband filters used throughout HST's history, such as F555W, F606W, and F814W, our exposure times are set to ensure a detection with  $S/N = 10$  two magnitudes below the main-sequence turnoff of NGC 2419. We also ensure such a detection in the other broad and long pass filters falling in this wavelength range, including F600LP, F625W, and F775W. These exposure times are typically 20-25 minutes each, and thus we use a  $CRSPLIT = 2$  with these sequences. The exposure time for F850LP is kept at 25 minutes, although the  $S/N$  will be lower in this filter at the same magnitude limit defined above.

Similar to these observations, we will also image 47 Tuc with WFC3 extending from the bright-blue main-sequence turnoff at  $V = 17.5$  to the faint-red part of the main-sequence approximately six magnitudes below the turnoff. This data set, spanning more than 1.5 magnitudes in  $V - I$  color, will nicely overlap both ground based photometry and the ACS calibration shown in Figure 2. These data will supplement the calibration described earlier and provide a check of the dependency of the photometric transformation equations on metallicity (47 Tuc is  $30\times$  more metal-rich than NGC 2419). Given the lack of hot horizontal branch stars in the cluster, the bluest filter that we will observe for this data set is F390W which alone requires almost one orbit to reach the desired  $S/N$ . For redder filters, the exposure times quickly decrease and multiple filters can be fit into single orbits.

The observations of both NGC 2419 and 47 Tuc require ten orbits to execute, and so the total program size is 43 orbits. Note, for a few of the star cluster observations, we have adjusted the actual integration times from the values listed above to efficiently fill the orbits and hide the buffer dumps. The photometric transformation aspect of our proposal has lower priority than the zeropoint goals, and therefore, should photometric stability require additional observations of the primary standards at finer cadence, the star cluster observations will be reduced or eliminated altogether.

## **IR – Spectrophotometric Standards and Star Clusters**

Similar to the UVIS photometric zeropoint plan, we will also execute additional observations with the WFC3/IR channel during Cycle 17 (i.e., as compared to SMOV). Here we briefly summarize the IR calibration plan as the justification for exposure times and choice of targets has already

been presented above.

The primary star is GD 153 although we will also obtain observations of both G191-B2B and GD 71. Each set of observations of a given standard, in all 15 of the IR filters, can be executed in a single orbit. These observations consist of a series of two point dither pattern exposures using the RAPID (broadband filters) and SPARS10 (medium and narrow-band filters) with the 128k, 256k, or 512k subarray. Additional observations with the broadband filters using a full frame readout are also included in each orbit (which defines a single visit). A second orbit (and grouped visit) is required to image the redder standard P330E in all filters, using a similar setup. Dither patterns are used to mitigate persistence (including a dark exposure after each set of observations) and exposure times are set to very small values (e.g.,  $<1$  second in broadband filters) using a small number (e.g., 1 or 2) of NSAMPS. Each observation will guarantee a  $S/N > 100$ .

We note that some of the observations of P330E and G191-B2B require a smaller subarray to avoid saturation in the readout. For these, we may have to bootstrap the total enclosed flux of the star from the full frame readout (e.g., translate the flux at some pixel to the total flux), or calibrate the subarray-full frame relation with fainter stars.

Finally, we will observe 47 Tuc in the five broadband filters using a full frame readout for the photometric transformation goals. These observations require two orbits and will achieve a depth  $>7$  magnitudes below the main-sequence turnoff, providing a rich sample of cluster stars with well measured photometry.

The observations of a given standard are repeated roughly once per month for the Cycle, requiring 13 grouped visits for a total of 26 orbits. Added to the star cluster observations, the program requires a total of 28 orbits.

## Analysis Plan

The analysis for the SMOV and Cycle 17 programs is virtually identical. We will use the processed files from the calwf3 pipeline at all times, and combine individual exposures with cosmic ray rejection. The light from these bright standards will subtend a large number of pixels on the detector. For all clean individual and combined data sets, we will construct profiles of the enclosed energy by measuring the flux in a large set of apertures of increasing radius. With ACS, the aperture radius at which the encircled energy was  $\simeq 100\%$  was  $5.5''$  (110 pixels). Aperture photometry will also require a background correction from an annuli exterior to this; ACS used  $6'' - 8''$  (120 – 160 pixels). Based on these numbers, and considering the similarities of ACS and WFC3, our  $512k \times 512k$  subarray should easily allow us to measure the full light profile of the standards on the UVIS channel. However, we will check for the true extent of the PSF wings in full frame readouts of UVIS1 and UVIS2 and of the IR detector.

Each star's curves of growth will be analyzed to measure the total flux (i.e., out to the radius

at which there is no light from the star) and aperture corrections will be constructed to extrapolate the flux at any aperture to the total flux. This is difficult for very small apertures and may require a PSF model as a function of position on the detector. These measurements are then compared to the expected count-rate of the calibration spectrum of the spectrophotometric standard, folded through our filter. The accuracy of this calibration depends on the modeling of spectral features in the observed stellar spectrum (hence the use of white dwarfs) and our understanding of the filter bandpasses. The results from this comparison will allow us to modify the sensitivity curves, to resolve any differences, and to update the ETC.

The photometric zeropoint of a filter is defined to be the magnitude of a star-like object that produces one count per second within the photometric aperture. This zeropoint can be tied to a specific photometric system within the approach we described above based on synthetic photometry (i.e., the measurement of magnitudes in a filter from the spectral energy distribution). For example, the VEGAMAG system is defined by setting the magnitude of the star Vega to zero in all bandpasses, whereas the STMAG and ABMAG systems are flux based, and are defined such that a certain flux density will have a magnitude of zero in all filters. As different users prefer different magnitude systems, we will calculate zeropoints in all three photometry systems. The observed brightness of an arbitrary star in that filter can then be simply calculated as  $2.5 \log(\text{total count-rate [e}^- \text{ s}^{-1}]) + (\text{specific zeropoint})$ .

For the analysis of the star cluster data, we will produce matched catalogs between our WFC3 broadband UVIS and IR observations to existing ground and space based data sets in several filter sets. This will include Johnson-Cousins *UBVRI* data, SDSS *u'g'r'i'z'* data, WFPC2 and ACS observations, and 2MASS *JHK* data. Coefficients for transformation equations will be calculated by relating the flux in the source band to the target band through an offset and color term (possibly second order). Of course, such comparisons will only be made for filters that are similar in the two bandpasses (e.g., F110W on WFC3/IR and the *J*-band on 2MASS). We expect this to be a difficult exercise for most filters given the expected lack of overlapping stars in the two catalogs (due to different brightness regimes and field of view), photometric errors in the ground based data, and the intrinsic understanding of the accuracy of the response function of the bandpasses. It is difficult to speculate how useful these comparisons may be for users until the datasets are in hand and analyzed. Further information on photometric transformations for ACS are described in Sirianni et al. (2005).

## Conclusions

In this short document we have described the observational and analysis plans for understanding the photometric calibration of the WFC3 UVIS and IR detectors. The observations will primarily consist of a set of very short, well-dithered snapshots of the HST spectrophotometric standards G191-B2B, GD 153, and P330E. These data will allow us to measure the photometric zeropoints of all wide, medium, and narrow-band WFC3 filters, as well as the narrow-band quad

filters that are being used in Cycle 17. We have also supplemented the standard star observations with images of 47 Tuc and NGC 2419 to define photometric transformations between the WFC3 UVIS and IR filters and other popular broadband systems. An extensive set of star cluster observations will also be obtained in other WFC3 calibration programs and Cycle 17 GO programs (e.g., 11729, Holtzmann et al. and 11664, Brown et al.) and will be used to provide additional leverage on our calibrations. A summary of these star cluster observations is provided in Sabbi et al. (2009)

Built into our observational plan is a cadence to measure the photometric stability of the detectors over the Cycle. We plan to make real-time adjustments to our observational strategy depending on the performance and our understanding of the detectors. For example, if excellent temporal stability can be established very early in Cycle 17, orbits for repeat observations of standard stars later in the Cycle can be shifted to other calibration goals, such as better defining the photometric transformations to other bands. Alternatively, the latter goals will be eliminated if further observations of standard stars (possibly including new standards) are required to understand any temporal variations in the detector that remain poorly understood from the initial set. A summary of all observations is presented in Tables 3 and 4.

Understanding the photometric performance of an instrument depends on many factors. For WFC3, many individual SMOV and Cycle 17 programs have been constructed to characterize a wide range of effects including charge transfer efficiency, flat-field errors, contamination, UVIS droplets, jitter from the shutter, fringing, bowtie, focus breathing, IR linearity, etc. Ultimately, the photometric calibration of WFC3 is not just related to this photometry program, but rather the interplay of all of these effects.

## Acknowledgements

We wish to thank E. Barker for reviewing this document and providing several helpful comments.

Table 3: Summary of WFC3 UVIS Photometric Calibration Program

Target	Filters	Cadence (months)	Subarray	Orbits
<b><u>UVIS Standards</u></b>				
GD 153 <sup>a</sup>	All Filters <sup>b</sup>	Once (early)	512×512 k	6
GD 153	F225W, F275W, F336W, F350LP F390W, F438W, F475W, F555W F850LP, F606W, F814W, F467M F547M, F469N, F502N, FQ906N	1, 2, 3, 5, 7, 9, 11, 13	512×512 k	16
GD 153	F225W, F336W, F350LP, F438W F555W, F606W, F814W	1, 2, 3, 5, 7, 9, 11 <sup>c</sup>	UVIS1/2	0 <sup>d</sup>
G191-B2B	F336W, F350LP, F390W, F438W F475W, F555W, F606W, F775W F814W, F850LP	1, 4, 7, 10, 13	512×512 k	5
P330E	F200LP, F218W, F225W, F275W F300X, F336W, F350LP, F390W F438W, F475W, F475X, F555W F600LP, F606W, F625W, F775W F814W, F850LP, F410M, F467M F547M, F621M, F689M	1, 6	512×512 k	6
<b><u>UVIS Clusters</u></b>				
NGC 2419	F200LP, F225W, F275W, F300X F336W, F350LP, F390W, F438W F475X, F475W, F555W, F600LP F606W, F625W, F775W, F814W F850LP	Once (middle)	Full Frame	5
47 Tuc	F390W, F438W, F475X, F475W F555W, F600LP, F606W, F625W F775W, F814W, F850LP	Once (middle)	Full Frame	4

<sup>a</sup>The same observations are scheduled for G191-B2B and GD71 if this target is unavailable.

<sup>b</sup>Excluding quad filters not being used in Cycle 17.

<sup>c</sup>One filter per visit, alternating between UVIS1 and UVIS2.

<sup>d</sup>Exposures are included in the above observations with the same cadence.



Table 4: Summary of WFC3 IR Photometric Calibration Program

Target	Filters	Cadence (months)	Subarray	Orbits
<b><u>IR Standards</u></b>				
GD 71	All Filters	1, 2, 7, 12, 13, 14	128, 256, 512k	6
GD 71	F105W, F110W, F125W F140W, F160W	1, 2, 7, 12, 13, 14	Full Frame	0 <sup>a</sup>
GD 153	All Filters	3, 4, 5, 6, 7, 8, 9, 10, 11	128, 256, 512k	9
GD 153	F105W, F110W, F125W F140W, F160W	3, 4, 5, 6, 7, 8, 9, 10, 11	Full Frame	0 <sup>a</sup>
G191-B2B	F110W, F105W, F140W, F125W	Once (middle)	128, 256k	1
G191-B2B	F098M, F160W, F127M, F139M F153M, G102, G141	Once (middle)	128, 256k	0 <sup>a</sup>
P330E	All Filters	1, 2, 4, 5, 6, 9, 10, 11, 12, 14	64×64 k	10
<b><u>IR Clusters</u></b>				
47 Tuc	F105W, F110W, F125W F140W, F160W	Once (middle)	Full Frame	2

<sup>a</sup>Exposures are included in the above observations with the same cadence.

## References

- Bergeron, P., Saffer, R. A., & Liebert, J. 1992, *ApJ*, 394, 228
- Bergeron, P., Liebert, J., & Fulbright, M. S. 1995, *AJ*, 444, 810
- Bohlin, R. C., Colina, L., & Finley, D. S. 1995, *AJ*, 110, 1316
- Bohlin, R. C. 1996, *AJ*, 111, 1743
- Bohlin, R. C. 2000, *AJ*, 120, 437
- Bohlin, R. C., Dickinson, M. E., & Calzetti, D. 2001, *AJ*, 122, 2118
- Bohlin, R. C. 2007, ACS ISR 2007-06, "Photometric Calibration of the ACS CCD Cameras"
- Brown, T. M., Hartig, G., & Baggett, S. 2008, WFC3 ISR 2008-10, "WFC3 TV3 Testing: UVIS Window Contamination"
- Lanz, T., Barstow, M. A., Hubeny, I., & Holberg, J. B. 1996, *ApJ*, 473, 1089
- Reid, I. N. 1996, *AJ*, 111, 2000
- Sabbi, E., et al. 2009, WFC3 ISR 2009-06, "WFC3 Calibration Using Galactic Clusters"
- Sirianni, M., et al. 2005, *PASP*, 117, 1049